EFFECTS OF LOADING RATE ON THE LOCAL CLEAVAGE FRACTURE STRESS σ_f IN NOTCHED SPECIMENS

G.Z. Wang,   Y.L. Wang and J.H. Chen

State Key Laboratory of New Nonferrous Metal Materials, Lanzhou University of Technology, Lanzhou 730050, China.

ABSTRACT

Four point bending (4PB) notched specimens with different notch sizes are tested at various loading rates at a temperature of -110^oC for a C-Mn steel. An elastic-plastic finite element method (FEM) is used to determine the stress distributions ahead of notches. By accurately measuring the distances of the cleavage initiation sites from the notch roots, the local cleavage fracture stress σ_f is measured, and the effects of loading rate and notch size on σ_f are investigated. The results show that the local cleavage fracture stress σ_f does not essentially change with loading rate and notch size. The reason for this is that the cleavage micromechanism does not essentially change in the different specimens at various loading rates. For the steel with low critical plastic strain for fracture initiation in this work, the cleavage micromechanism involves competition of two critical events of crack propagation and crack nucleation in the high stress and strain volume ahead of notch root. For the tested steel, the critical events in the specimens which the cleavages are directly initiated at the notch tips are mainly the propagation of a ferrite grain-sized crack controlled by tensile stress, and the critical events in the specimens which the cleavages are initiated at a distance from the notch root are mainly crack nucleation controlled by plastic strain. The large scatter of σ_f and notch toughness are mainly caused by the different critical events in different specimens. The measured σ_f values and notch toughness corresponding to the critical event of crack propagation are lower than that of crack nucleation.

1   INTRODUCTION

It is well known that the cleavage fracture of ferritic steels is controlled by a critical local tensile stress criterion (σ_{yy} σ_f) [1]. A salient feature of cleavage fracture is the variability of experimental results. An extensive scatter band of measured values is usually observed for global parameters assessing fracture toughness such as K_{1c}, J_{1c} and COD. A lot of probabilistic models have been developed to describe the distribution of measured scatter values [2,3]. Most models are based on the weakest link theory, i.e. the whole specimen fails at the moment when the normal stress σ_{yy} exceeds the local fracture stress σ_f and propagates a cleavage crack in a carbide particle. Therefore, σ_f is an important parameter for the cleavage fracture models. It is considered to be nearly independent of test temperature [4], notch sizes [5] and specimen sizes [6], is taken as a fracture

parameter connecting the macroscopic fracture toughness with the microstructure of metal material [4,7].

However, the effects of loading rate on σ_f have not been completely validated. In previous work [4], σ_f values estimated from Charpy V impact test are essentially the same as that measured by 4PB specimens tested at quasi-static loading, thus it is considered that the $_f$ is nearly independent of loading rate. In this work, the σ_f values are accurately measured by 4PB tests of notched specimens with different notch sizes and the FEM calculation of stress distribution ahead of the notches at various loading rates. The effects of loading rate and notch size on σ_f are investigated. Micromechanism of cleavage fracture is also demonstrated from experimental results.

2   EXPERIMENTAL PROCEDURES

2.1 Materials, specimens and experiments

A C-Mn vessel steel was used. The composition (wt%) of the steel is C=0.18, Mn=1.49, Si=0.36, S=0.03, and P=0.01, and the microstructure is composed of ferrite and pearlite. Tensile and four point bending (4PB) specimens are cut in the steel. Two types of 4PB specimens (4V and 4I) with single-notch and double-notch are used. The 4V and 4I specimens have the same thickness W =12.7mm, width B =12.7mm and notch depth a = 4.25mm, but different notch flank angle and notch root radius . The notch flank angle and notch root radius of the 4V specimen (=90° ,   = 0.25mm) are larger than that of the 4I specimen (=0° ,   = 0.14mm). The double notch specimens are used for observing the remaining micro cracks.

Tensile and 4PB tests were carried out at different loading rates of 1, 60, 120, 240, 360 and 500mm/min at −110°C. The fracture load P_f and the absorbed energy E for fracture (the area covered by the load – displacement curve) in the 4PB test were measured by the load – displacement curve. Fracture surfaces of all 4PB specimens were observed in detail with a scanning electron microscope (SEM). The initiation site of cleavage fracture was located by tracing the river pattern strips back to their origin. The distance of the cleavage initiation site from the tip of the blunted notch was measured as X_f. For doubly notched specimens, fracture occurred at one notch and the critical condition was reached in the vicinity of the survived notch. The six metallographic sections perpendicular to the survived notch root were cut, and were grouped together in a single bakelite mount and polished using standard metallographic techniques.   The metallographic sections were etched with 2% natal to observe the remaining crack and identify the critical event of cleavage using the SEM [4,5,6].

2.3. Finite Element Method (FEM) calculation and measurement of the local cleavage fracture stress σ_f

The maximum normal stress σ_{yy} on the plane directly ahead of the notches were calculated. A two dimensional model with 4-node biquadratic plane strain reduced integration elements (CPE4R) was used with the ABAQUS/Explict code. The stress-strain response of the material at different loading rates (measured by the tensile test) obeys the power-hardening relation $\sigma = K\varepsilon^n$. The stress-strain curves at various strain rates were digitized and fit into the series of data for the input file of the FEM code. The various strain rates from the tensile tests were automatically used in different locations ahead of the notch by the FEM code in the FEM simulations.

At a measured fracture load P_f, corresponding curves of tensile stress σ_{yy} can be selected from the FEM calculation results. With the measured X_f (the distance of the cleavage initiation site from the tip of the blunted notch) as the abscissa, the corresponding ordinate value of the normal stress σ_{yy} of the stress distribution curve was taken as the local cleavage fracture stress σ_f.

3 RESULTS

Figures 1 summarizes the variations of notch toughness (characterized by the ratio of the fracture load to the general yield load, P_f/P_{gy}, and the absorbed energy for fracture, E) against the loading rate V for 4V and 4I specimens. In some 4V specimens with various loading rates, the distance X_f from the cleavage initiating site to the notch root is zero. In this case the cleavages are directly initiated at the notch tips, as typically shown in Figure 2(a). In the other 4V specimens the values of X_f are in a range of 96 - 1269μ m. This means that the cleavages are initiated at various distances ahead of notch root at various loading rates, as typically shown in Figure 2(b). In metallographic sections of fractured doubly notched specimens with various loading rates, the remaining cracks mainly limiting in ferrite grains with a length of 10 - 40μ m were found in a range of $X = 0$-80μ m close to notch roots, and the most cracks are located at notch tips ($X = 0$), and some of them is blunted, as typically shown in Figure 3. In the range larger than 80μ m away from the notch root, no remaining cracks were found. The cleavage initiation behavior of the 4I specimens is similar to that of the 4V specimens. Figure 4 shows the variation of the σ_f measured in 4V and 4I specimens with loading rate V. All σ_f values of the 4V and 4I specimens are in the same scatter range of 1000 – 1500MPa. This means that the local cleavage fracture stress σ_f does not essentially change with loading rate V and notch size. The σ_f values corresponding to $X_f = 0$ are lower than that corresponding to $X_f \neq 0$.

(a)   (b)
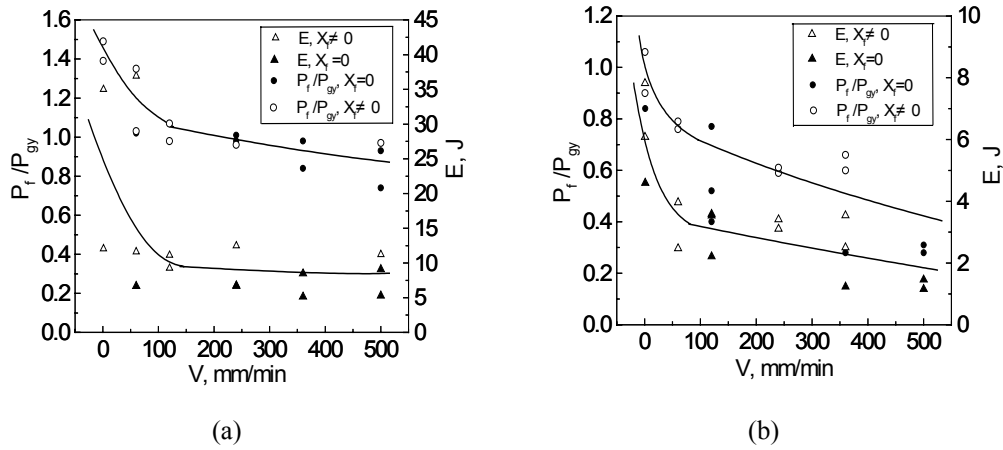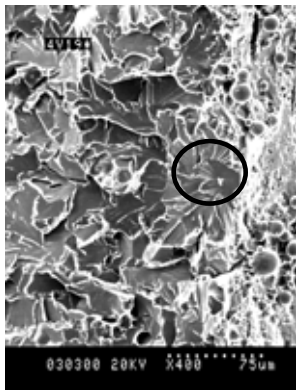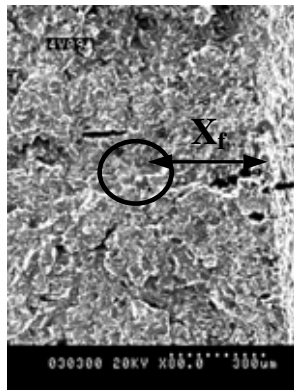
Figure 1: The variations of notch toughness against loading rate V for 4V (a) and 4I (b) specimen

(a)   (b)
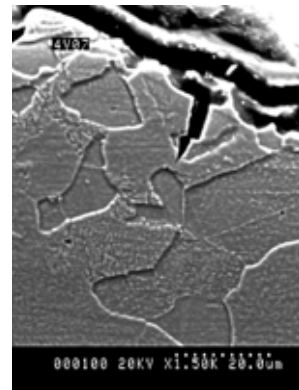
Figure 2: Typical fracture surfaces for 4V specimen

Figure 3: Typical ferrite grain-sized remaining microscopic cracks

4   DISCUSSION

Figure 4 shows that the local cleavage fracture stress σ_f does not essentially change with loading rate V and notch size, and has a large scatter for this steel. This could be analyzed as follows:

According to the works in Ref.[8],   the σ_f is mainly determined by the critical event of the cleavage fracture. The characteristic feature of a critical event of crack propagation controlled by tensile stress is that the cracks limiting in the microstructural domain that nucleated but failed to

propagate remain in a fractured specimen. That a crack remains in front of the surviving notch means the tensile stress was not sufficient to propagate the crack just nucleated. This shows a tensile stress-controlling crack propag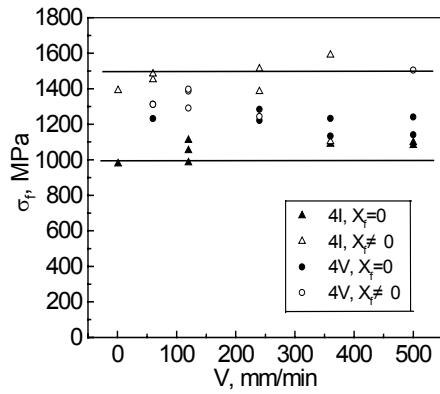ation mechanism. However, the characteristic feature of a critical event of crack nucleation is that no remaining crack can be found in the corresponding range of cleavage initiation sites (X_f) ahead of notch root in fractured specimens.

Figure 4: The local cleavage fracture Stress σ_f of the 4V and 4I specimens

For the steel with low critical plastic strain for fracture initiation [6] in this work the microscopic observations show that for some 4V and 4I specimens tested at various loading rates the cleavages are directly initiated at the notch tips ($X_f = 0$) (Figure 2(a)), and many remaining cracks limiting in ferrite grains were also found at notch tips ($X = 0$) (Figure 3). These facts indicate that the critical events in these specimens with $X_f = 0$ are mainly the propagation of a ferrite grain-sized crack controlled by tensile stress. However, for the 4V and 4I

specimens with X_f 0, the cleavages were initiated in a range of $X_f = 96 - 1269\mu$ m and $X_f = 195 – 447\mu$ m, and no remaining cracks were found in the range (the corresponding range of cleavage initiation site X_f) larger than 80μ m away from the survived notch root of the fractured doubly notched specimen. These facts means that the critical events in these specimens with X_f 0 are mainly crack nucleation controlled by plastic strain. Therefore, two cleavage mechanisms corresponding to two critical events of crack propagation and crack nucleation seem to compete in the high stress and strain volume ahead of notch roots. While the loading rate and notch size varies, the two critical events in the two types of specimen (4V and 4I) do not change, that is, the two cleavage micromechanisms do not change in the different specimens. This can be considered as the microscopic reason for the independence of the σ_f on loading rate and notch size. The large scatter of σ_f in Figure 4 and the large scatter of notch toughness in Figure 1 are mainly caused by the different critical events in different specimens. The measured σ_f values (Figure 4) and notch toughness (Figure 1) corresponding to the critical event of crack propagation ($X_f = 0$) are lower than that of crack nucleation (X_f 0).

5   CONCLUSION

(1) The local cleavage fracture stress σ_f does not essentially change with loading rate V and

notch size. The reason for this is that the cleavage micromechanism does not essentially change in the different specimens at various loading rate.

(2) For the steel with low critical plastic strain for fracture initiation in this work, the cleavage micromechanism involves competition of two critical events of crack propagation and crack nucleation in the high stress and strain volume ahead of notch root. The critical events in the specimens which the cleavages are directly initiated at the notch tips ($X_f = 0$) are mainly the propagation of a ferrite grain-sized crack controlled by tensile stress, and the critical events in the specimens which the cleavages are initiated at a distance from the notch root ($X_f \quad 0$) are mainly crack nucleation controlled by plastic strain.

(3) The large scatters of σ_f and notch toughness are mainly caused by the different critical events in different specimens. The measured σ_f values and notch toughness corresponding to the critical event of crack propagation are lower than that of crack nucleation ($X_f \quad 0$).

REFERENCES

[1] Ritchie RO, Knott JF, Rice JR. On the relationship between critical tensile stress and fracture toughness in mild steel. Journal of the Mechanics and Physics of Solids, vol.21, pp.395-410, 1973.

[2] Beremin FM. A local criterion for cleavage fracture of a nuclear pressure vessel steel. Metallurgical Transactions, vol.14A, pp.2277-2287, 1983.

[3] Gao X, Dodds RH, Jr, Tregoning RL, Joyce JA. Weibull stress model for cleavage fracture under high-rate loading. Fatig & Fract Engng Mater & Struct, vol.24, pp.551-564, 2001.

[4] Chen JH, Wang GZ, Yan C, Ma H, Zhu L. Advances in the mechanism of cleavage fracture of low alloy steel at low temperature. Part : local fracture stress σ_f . International Journal of Fracture, vol. 83, pp.139-157, 1997.

[5] Wang GZ, Wang HJ, Chen JH. Effects of notch geometry on the local cleavage fracture stress σ_f. Fatigue and Fracture of Engineering Materials and Structures, vol.22, pp.849-858, 1999.

[6] Wang GZ, Wang JG, Chen JH. Effects of geometry of notched specimens on the local cleavage fracture stress σ_f of C-Mn steel. Engineering Fracture Mechanics, vol. 70, pp.2499-2512, 2003.

[7] Samant AV, Lewandowski JJ. Effects of test temperature, grain size, and alloy additions on the cleavage fracture stress of polycrystalline niobium. Metallurgical and Materials Transactions, vol.28A, pp.389-399,1997.

[8] Curry DA, Knott JF. Effect of microstructure on cleavage fracture stress in steel, Materials Science, Nov, pp.511-514. 1978.